Design of Multiband Metamaterial Microwave BPFs for Microwave Wireless Applications

Ahmed Hameed Reja and Syed Naseem Ahmad

Abstract. This work proposes an end-coupled half wavelength resonator dual bandpass filter (BPF). The filter is designed to have a 10.9% fractional bandwidth (FBW) at center frequency of 5.5GHz. Dual-band BPF with more drastic size reduction can be obtained by using metallic vias act as shunt-connected inductors to get negative permittivity (-ε). The process of etching rectangular split ring resonators (SRRs) instead of open-end microstrip transmission lines (TLs) for planar BPF to provide negative permeability (-μ) is presented. The primary goals of these ideas are to get reduction in size, dual- and tri- bands frequency responses. These metamaterial transmission lines are suitable for microwave filter applications where miniaturization, dual- and tri-narrow passbands are achieved. Numerical results for the end-coupled microwave BPFs design are obtained and filters are simulated using software package HFSS. All presented designs are implemented on the Roger RO3210 substrate material that has; dielectric constant ε_r=10.8, and substrate height h =1.27 mm.

Keywords: Bandpass filter, end coupled, metamaterial, microwave, multiband, split ring resonator.

1 Introduction

Microwave bandpass filters are vital components in a wide range of microwave systems, including satellite communications and radar. Transmission line resonator structures consist of a combination of multi-lines of at least one quarter guide

Ahmed Hameed Reja
Department of Electromechanical Engineering,
University of Technology, Baghdad, Iraq

Ahmed Hameed Reja · Syed Naseem Ahmad
Department of Electronics & Communication Engineering
Jamia Millia Islamia, New Delhi-110025, India
e-mail: ahmad8171@yahoo.com, snahmad@jmi.ac.in

El-Sayed M. El-Alfy et al. (eds.), *Advances in Intelligent Informatics*,
Advances in Intelligent Systems and Computing 320, DOI: 10.1007/978-3-319-11218-3_18

wavelength ($\lambda_g/4$), these structures are used as components in different types of filters with different filtering characteristics.

The most popular of various design structures for RF/microwave filters include end-coupled, edge-coupled, hairpin and interdigital filters. Fig. 1 shows a third order end-coupled microstrip filter [1].

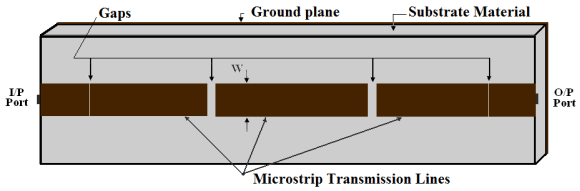

Fig. 1 Three poles end-coupled bandpass filter structure

End-coupled line filters consist of open-end microstrip resonators of approximately half wavelength. The resonators are coupled between them through a gap-spacing (S) for designing of bandpass filters. But it has the disadvantage of consumes more space compared to other microwave filters. In planar technology, filters with small fractional bandwidth (FBW) could be implemented in case of end-coupled resonators, since the coupling between resonators have to be weak. So, this topology cannot be used for the design of wider band filter [1]. There are many advantages of this type of filter such as; low cost, fairly high tolerance, and ease of fabrication. To miniaturize the filter size, the metamaterial idea is presented in this paper. Metamaterials (MTMs) are defined as artificial, effectively homogeneous (average cell size p is much smaller than the guided wavelength, λ_g) and exhibiting highly unusual properties (negative values of effective permittivity ε_r, and effective permeability μ_r) not readily available in nature [2, 3].

The electromagnetic properties of metamaterials were already predicted by Veselago in 1968 [2]. Split-ring resonators (SRRs) were one of the first particles for metamaterial structure which were proposed by Pendry in 1999 [4]. The metallic metamaterials comprises double SRRs are the main artificial structures to realize magnetic responses above gigahertz frequencies [5, 6, 7, 8]. The double SRRs topologies depicted in Fig. 2 are used to obtain a negative value of effective

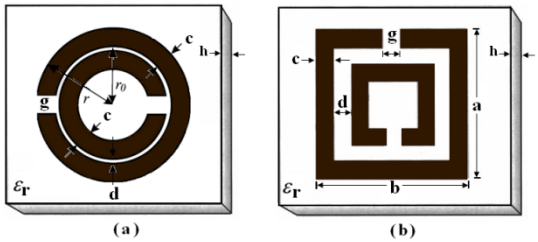

Fig. 2 SRR topologies (a) circle shape, (b) square shape. The relevant dimensions are indicated. (Metal regions are depicted in brown color)

permeability over a desired frequency range. In planar technology, one-dimensional left handed metamaterials and negative permeability transmission lines based on SRRs have been proposed [9, 10].

A dual-band, tri-band and quad-band as a multiband of frequencies are necessary in telecommunication applications. All communication devices which have many channels use multiband frequencies. The need for the design of compact, low-cost, and robust radio frequency (RF) devices operating at multiband frequency to facilitate and develop the next generation wireless systems. These devices are used rather than; complexity, high cost and power demand of multiband parallel transmit and receive signal path circuits. In literature, there are various approaches reported for dual- and tri- bands of BPFs. All these approaches depend on the change of substrate material parameters such as thickness and dielectric constant or change of geometrical parameters of resonators such as unit cell dimensions, strip and split widths, gap widths and separation between the rings. The design of planar dual-band BPFs using modified SRRs as a metamaterial component is presented. The resonance frequencies are analytically derived, and the field distribution on each SRR is studied [11]. A dual-band microstrip filter depending on double resonant property of the complementary split ring resonators (CSRRs) as a resonant unit and T-shaped stub as feeding structure is designed. This filter has two passbands of (2.4 - 2.6) GHz and (3.8 - 4.3) GHz with low insertion loss inside band and high rejection out-of-band [12]. A compact dual-band microstrip filter with equal-length SRRs and zero degrees-feed structure is proposed. A zero degrees-feed structure is applied to realize additional transmission zeros at finite frequencies [13]. A miniaturized dual-band BPF module using double-split (DS)-CSRR and SRR is presented. Two passbands are individually printed on two sides of a substrate material (Rogers 3010) as a compact integration [14].

A compact dual-band BPF using side-coupled octagonal SRRs is proposed. The filter employs two sets of SRRs operating at different frequencies to generate two passbands and provide facilities to control the bandwidth of the two passbands [15]. A compact dual-band substrate integrated waveguide (SIW) filters based on two different types of CSRRs loaded on the waveguide surface is presented. Compact size, good selectivity, stopband rejection and easy fabrication are achieved [16]. A dual-band BPF using SRRs and defected ground structure (DGS) with constant absolute bandwidth is proposed. The inner and outer SRRs are operated for respective passband. DGS can control the coupling coefficient of the filter. This kind of filter with compact size and high selectivity is designed and fabricated [17]. Three SRRs used to obtain a triple-band response is proposed. Two topologies to design triple-band filters with controllable responses and a systematic filter design approach based on a filter coupling model are presented [18]. Miniaturized multiband filters using CSRRs is proposed. A multiple passbands can be generated by loading different types of CSRRs on the waveguide surface. Two types of dual-band filters, a triple-band and a quadruple-band filter are designed and fabricated. The advantages of these filters are compact size, good selectivity and high stopband rejection [19]. A technique based on combination

of two parallel multimode resonators and single CSRR to design multi-notch bands ultra-wideband (UWB)-BPF is discussed. The mechanism of realizing the notch-bands is mathematically presented and a triple notch-bands UWB-BPF is designed, simulated and fabricated. The size reduction of around 35% is demonstrated compared to the conventional filter [20].

In this paper, an end-coupled dual- and tri- bands microwave BPF design has been presented. Dual-band filter with size reduction can be obtained by using vias. To enhance the magnetic coupling and obtain multiband, the preferred structure used is etching rectangular SRRs instead of traditional open ended transmission lines at same external dimensions. It will be shown that the designed metamaterial structures can found applications to the design of dual- and tri-bands microwave filters. These metamaterial structures interest in compact microwave filters design used in wireless applications.

2 End-Coupled, Half-Wavelength Resonator Filter Design

2.1 Traditional End-Coupled Filter Design

Fig. 3 shows the general configuration of three poles (n = 3) end-coupled microstrip BPF, where each open-end microstrip resonator is approximately a half guided wavelength ($\lambda_g/2$) long at the resonant frequency (f_o) of the bandpass filter. A microstrip gap (S) can be represented by an equivalent circuit, as illustrated in Fig. 4 [21].

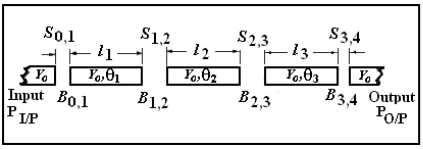

Fig. 3 Three poles configuration of end-coupled microstrip BPF

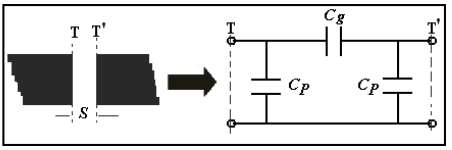

Fig. 4 Microstrip gap and its equivalent circuit

The shunt (C_p) - and series (C_g) - capacitances may be determined by using equations in [22]. These capacitances depend on the width of microstrip (W), dielectric constant of substrate material (ε_r), gap between two adjacent resonators (S), and the thickness of substrate material (h).

$$C_p^{j,j+1}=0.5\ C_e^{j,j+1} \tag{1}$$

$$C_g^{j,j+1}=0.5C_o^{j,j+1}-0.25C_e^{j,j+1} \tag{2}$$

The components C_o and C_e are expressed as

$$\frac{C_o^{j,j+1}}{W}=\left(\frac{\varepsilon_r}{9.6}\right)^{0.8}.\left(\frac{S_{j,j+1}}{W}\right)^{m_o}.e^{k_o} \qquad \left(^{PF}/_{m}\right) \tag{3}$$

$$\frac{C_e^{j,j+1}}{W}=12\left(\frac{\varepsilon_r}{9.6}\right)^{0.9}.\left(\frac{S_{j,j+1}}{W}\right)^{m_e}.e^{k_e} \qquad \left(^{PF}/_{m}\right) \tag{4}$$

where

$$m_o=\frac{W}{h}\left[0.619.\log(W/h)-0.3853\right] \quad \text{for } 0.1\le s/W\le 1 \tag{5}$$

$$k_o=4.26-1.453.\log(W/h)$$

$$m_e=0.8675 \quad \text{for } 0.1\le s/W\le 0.3 \tag{6}$$

$$k_e=2.043(W/h)^{0.12}$$

The capacitive coupling in open-ends from one resonator structure to the other is through the gap between them, this gap can be represented by J- inverters, which are of the form in Fig. 5 [21]. These J-inverters go about to reflect high impedance levels to the ends of each resonator, and this causes the resonators to exhibit a shunt-type resonance [23]. A third order (n = 3) Chebyshev low pass filter (LPF) prototype with a normalized cutoff Ω_c = 1 and 0.1dB passband ripple is chosen. Whose order of the filter and element values (g_n) are listed in Table 1.

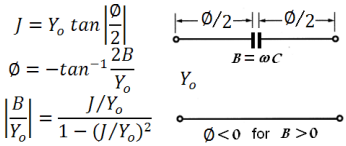

Fig. 5 J-inverters with respect to lumped and transmission line elements

Table 1 The order of filter with element values

n	g_o	g_1	g_2	g_3	g_4
3	1	1.0316	1.1474	1.0316	1

A microstrip end-coupled BPF is designed to have a fractional bandwidth (FBW) of 10.9% at 5.5 GHz central frequency (f_o) related to upper (ω_2) and lower (ω_1) cutoff frequencies and expressed as [21].

$$FBW=\frac{\omega_2-\omega_1}{\sqrt{\omega_1.\omega_2}} \tag{7}$$

Thus, the filter under consideration operates as a shunt-resonator. The $J_{j,j+1}$ are the characteristic admittances of J-inverters and Y_0 is the characteristic admittance of the microstrip line. Whose general design equations are given as follows [21].

$$\frac{J_{01}}{Y_0}=\sqrt{\frac{\pi.FBW}{2.g_o.g_1}} \tag{8}$$

$$\frac{J_{j,j+1}}{Y_0} = \frac{\pi.FBW}{2.\sqrt{g_j.g_{j+1}}}, \qquad j=1 \text{ to } n-1 \tag{9}$$

$$\frac{J_{n,n+1}}{Y_0} = \sqrt{\frac{\pi.FBW}{2.g_n.g_{n+1}}} \tag{10}$$

The susceptance $B_{j,j+1}$ under perfect series capacitance condition for capacitive gaps act as in Fig. 5 and expressed as

$$\frac{B_{j,j+1}}{Y_o} = \frac{\frac{J_{j,j+1}}{Y_o}}{1-(\frac{J_{j,j+1}}{Y_o})^2} \tag{11}$$

The electrical lengths of half wavelength resonators are expressed as

$$\theta_j = \pi - \frac{1}{2}\left[\tan^{-1}\left(\frac{2B_{j-1,j}}{Y_o}\right) + \tan^{-1}(\frac{2B_{j,j+1}}{Y_o})\right], \quad \text{radians} \tag{12}$$

The effective lengths of the shunt capacitances on the both ends of resonators with guided wavelength (λ_{go}) and angular frequency ($\omega_o = 2\pi.f_o$) can be found by using the following expressions.

$$\Delta l_j^{e1} = \frac{\lambda_{go}.\omega_o.C_P^{j-1,j}}{2\pi.Y_o} \tag{13}$$

$$\Delta l_j^{e2} = \frac{\lambda_{go}.\omega_o.C_P^{j,j+1}}{2\pi.Y_o} \tag{14}$$

The physical lengths of resonators are given by [21]

$$l_j = \frac{\lambda_{go}.\theta_j}{2\pi} - \Delta l_j^{e1} - \Delta l_j^{e2} \tag{15}$$

2.2 Filters Simulation

For microstrip filters simulation, a substrate material with a relative dielectric constant ε_r = 10.8, substrate height h = 1.27mm and conductor thickness t = 0.035mm. The line width for microstrip half-wavelength resonators is also chosen W = 1.85mm. The simulation was conducted using high frequency structure simulator (HFSS) software package. The procedure design of end-coupled filter has been completed, and the final results are listed in Table 2 depending on Fig. 3. The layout dimensions of this design are (10.8mm x 32.411mm).

Table 2 The dimensions of filter components

W (mm)	$S_{0,1} = S_{3,4}$ (mm)	$S_{1,2} = S_{2,3}$ (mm)	$l_1 = l_3$ (mm)	l_2 (mm)	l ($P_{I/P}$=$P_{O/P}$) (mm)
1.85	0.057	0.52	8.15	8.7	3.123

Several width values of strip lines were taken so as to know which is better to get suitable results of filter design at the desired frequency. It is noted that the preferable value is 1.8mm or 1.85mm. Fig. 6 and Fig. 7 show the return (S_{11}) and insertion (S_{21}) losses frequency response, respectively and related to width of strip line. The return losses are 30dB in the first resonance at 5.5GHz and 20dB in the second resonance at 10.5GHz. The insertion losses at same points of resonances approach to 0.1dB and 2dB, respectively. One of the important parameters in filter design is the group delay, which is expressed as [21].

$$\tau_d = \frac{d\emptyset_{21}}{d\omega} \qquad \text{Seconds} \tag{16}$$

Where, $\emptyset_{21}$is the phase angle of S_{21} in radians, and ω is an angular frequency in radians per second. Fig. 8 shows the group delay for different microstrip width values, and it is observed that the group delay remains almost constant out of the passband interval and approximate to 0.12*n*s, whereas in the passband interval there is a sharp rise in group delay.

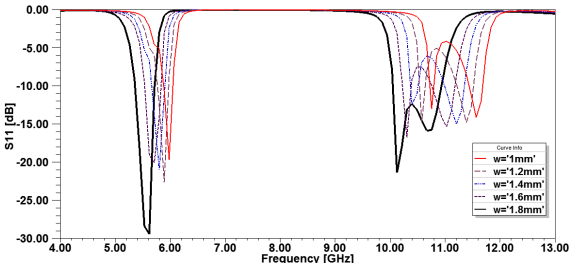

Fig. 6 Return loss responses (S_{11}) of BPF

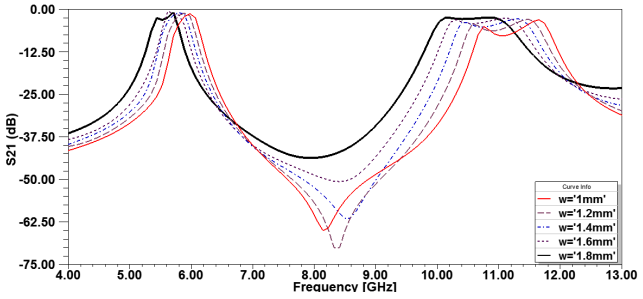

Fig. 7 Insertion loss responses (S_{21}) of BPF

Finally the simulated (through HFSS software, including losses) frequency response of the BPF with better results by taking 1.85mm width of strip line is shown in Fig. 9. The central frequency (f_o) of the filter is 5.5GHz and fractional bandwidth (FWB) equal to 10.9%, and the other resonance at 10.5GHz has FWB of 11.45%.

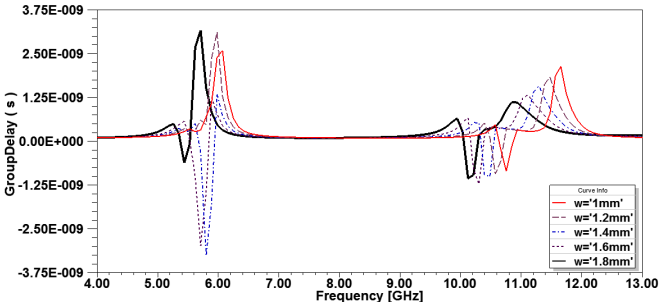

Fig. 8 Group delay variation in different microstrip width values of BPF

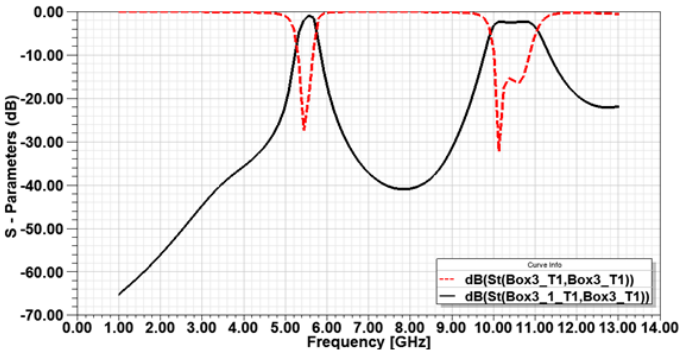

Fig. 9 Frequency response of dual-band BPF

Fig. 10 shows the group delay for dual-band BPF design and it is observed that the group delay remains almost constant out of the passband interval and approximate to 0.12*n*s, whereas the sharp rise in passband interval.

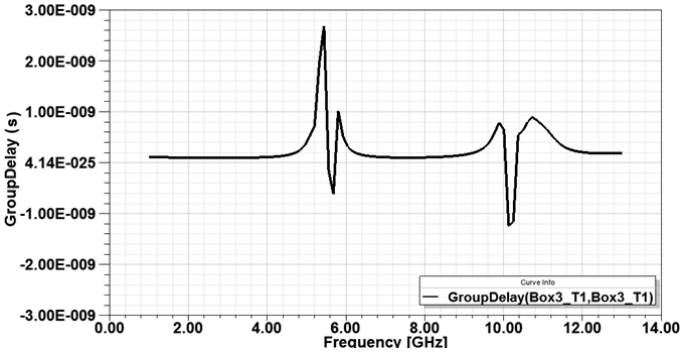

Fig. 10 Group delay variation for conventional dual-band BPF

3 Metamaterial Structures

3.1 Via Structure

In filter design more size reduction and dual-band frequencies can be obtained by using metallic vias at periodic positions. This metallic vias act as shunt-connected inductors, whereas metallic vias provide the required negative permittivity ($-\varepsilon_r$). Fig. 11 shows the geometric design of via intersects the upper conductor and the ground plane. The radius (r) of via in this design is equal to $0.005\lambda_g$.

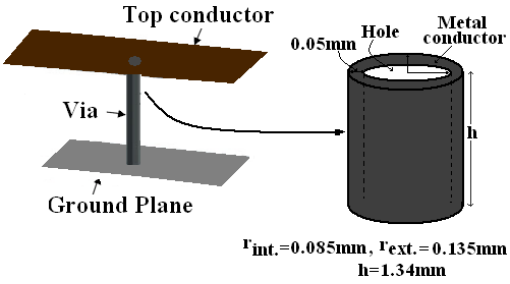

Fig. 11 Geometric design of via structure

3.2 Rectangular SRR Structure

The double SRR structure and its equivalent circuit are shown in Fig. 12. This structure is etching instead of an open-ended transmission line which acts as a shunt capacitance to get miniaturization and multiband resonances. In the double ring configuration, capacitive coupling (C'_1, C'_2) and inductive coupling (L'_1, L'_2) between the external and internal rings were connected by a coupling capacitance (C_m) and a transformer that has transformed ratio (T) [3].

The electromagnetic properties of SRRs structure were studied [4]. The SRRs structure has a negative permeability at specific resonant frequency (f_o) and can be calculated in case of circle shape SRRs as follows

$$\mu_{eff} = \frac{\pi r^2/A^2}{1+\frac{2l.\sigma}{w.r.\mu_o} i - \frac{3l.c_o}{\pi w^2 \ln\frac{2c.r^3}{d}}} \tag{18}$$

Where σ is the resistance per unit length, A, *l*, are the periods of z- and y-directions, respectively, and c_o is the light velocity. Thereafter changing from circle type parameters to rectangular type parameters with many approximations to get SRRs used in our design as shown in Fig. 12.

The external dimensions of rectangular SRRs have the same external dimensions of open-ended transmission lines. The rectangular type parameters for all resonators are (g = 0.15mm, d = 0.145mm, and c = 0.15mm). The lengths of internal resonators (r_1 and r_2) can be calculated easily from upper parameters.

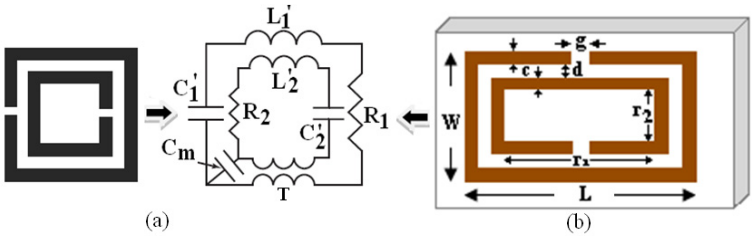

Fig. 12 SRRs topology a) Structure and equivalent circuit model b) Rectangular SRR

4 Metamaterial BPF

To obtain good electrical performances from the proposed filters, the design parameters were tuned and optimized using HFSS software based on finite element method. The layout of conventional filter is modified to get metamaterial filters with new results.

4.1 BPF Using Vias

The end-coupled microstrip poles are connected to the ground plane through metallic vias at periodic positions as shown in Fig. 13. This metallic vias act as shunt-connected inductors, whereas the distance between two adjacent vias is 8.95mm, and the internal radius of each via equal to 0.085mm.

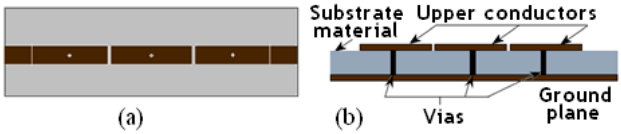

Fig. 13 End-coupled filter design contains vias (a) front view, (b) side view

The frequency response of this filter is shown in Fig. 14. We see that the new resonant frequencies are created in 3.58GHz and 5.58GHz respectively, and rejected at 10.5GHz. The return loss at new resonance frequencies are 22dB and 18dB, respectively. Fig. 15 shows the group delay and it is observed that the group delay remains almost constant approximate to 0.1*n*s along the stop-band interval, whereas beyond the passband there is a sharp rise in group delay.

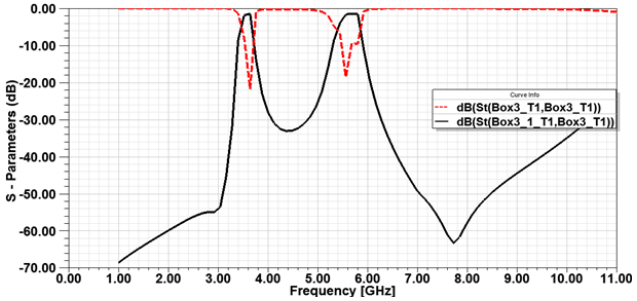

Fig. 14 Frequency response of dual-band BPF contains metallic vias

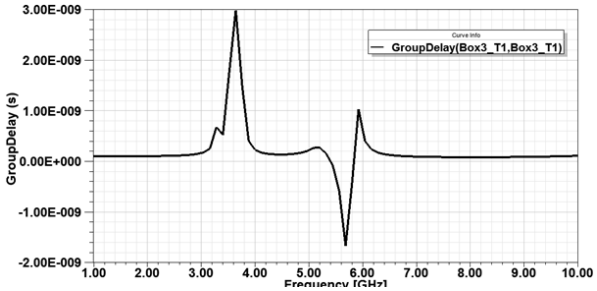

Fig. 15 Group delay of dual-band BPF contains metallic vias

4.2 BPF Using SRRs

The modification of end-coupled filter based on SRRs concept is shown in Fig.16. This idea is achieved by etching rectangular SRRs instead of open-ended transmission lines (l_1, l_2, l_3) in a conventional filter design to get reduction in size up to 20%, and tri-band frequencies at 4.4GHz, 7.9GHz, and 10.5GHz. Compact, low-cost and robust multiband microwave components are obtained when many communication standards are collected in one microwave wireless device. The disadvantage of this design is low return losses and less FBW compared to conventional counterpart. Fig.17 shows the frequency response of modified end-coupled filter. Fig.18 shows the group delay variation of the tri-band filter, and it is observed that the group delay remains almost constant out of the passband interval and approximate to 0.12*n*s.

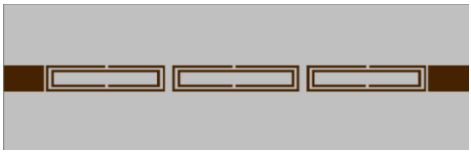

Fig. 16 Layout of three pole microstrip end-coupled split ring resonators filter

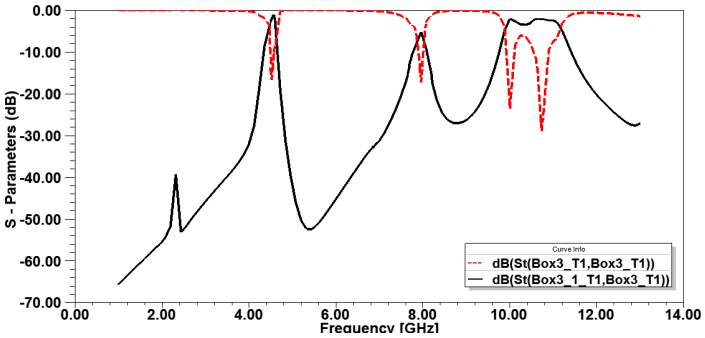

Fig. 17 Frequency response of tri-band filter contains SRRs

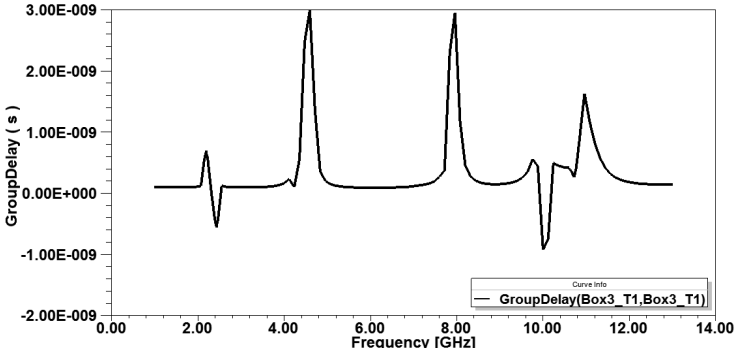

Fig. 18 Group delay variation of tri-band filter Contains SRRs

The comparison between traditional and metamaterial filters with respect to resonance frequencies, fractional bandwidths and return losses are listed in Table 3.

Table 3 Comparison between conventional and metamaterial filters

Filter type	Resonance frequency (GHz)			FBW %	RL (dB)
	f_{o1}	f_{o2}	f_{o3}	at f_{o1}, f_{o2}, f_{o3} respectively	
Conventional	5.5	-	10.5	10.9, -, 11.45	28, -, 18
Metamaterial -Vias	3.58	5.58	-	7, 8, -	22, 18, -
Metamaterial-SRRs	4.4	7.9	10.5	8.7,3.9,12.35	16, 17, 16

5 Conclusions

The end-coupled, half wavelength resonator, bandpass filter is presented for the first time in this paper. A new design achieved by using vias act as shunt inductors between microstrip lines and the ground plane. This idea gives a reduction in size and dual-band frequencies at lower and upper resonance frequency in conventional one. The MTM microstrip lines as periodic SRRs with deliberately

manufactured gaps between them have been designed. The main contribution of this work is that proposed structure can be used as a narrow bandpass filter with reasonably good performance. The group delay of BPFs remains almost constant out of the passband interval and is approximately 0.12*n*s. The advantages of the end-coupled resonator type of filters that they are fairly high tolerance, ease of fabrication and low cost. The disadvantages are that they consume more space and cannot be used for the design of wideband filters. After modification, more advantages are obtained, such as reduction in size, dual- and tri-bands frequency responses, but it exhibits low return losses at resonance frequencies and less value of fractional bandwidth (FBW*)* in the first resonance frequencies.

Acknowledgments. The authors would like to express their appreciation to the Ministry of Higher Education and Scientific Research in Iraq and Jamia Millia Islamia in India for supporting this work.

References

1. Lembrikov, B.: Ultra Wideband. Sciyo, Croatia (2010) ISBN 978-953-307-139-8
2. Veselago, V.G.: The electrodynamics of substances with simultaneously negative values of ε and μ. Sov. Phys. Usp. 10, 509–514 (1968)
3. Caloz, C., Itoh, T.: Electromagnetic Metamaterials: Transmission Line Theory and Microwave Applications. Wiley, Hoboken (2006)
4. Pendry, J.B., Holden, A.J., Robbins, D.J., Stewart, W.J.: Magnetism from conductors and enhanced nonlinear phenomena. IEEE Trans. Microwave Theory Tech. 47(11), 2075–2084 (1999)
5. Yen, T.J., Padilla, W.J., Fang, N., Vier, D.C., Smith, D.R., Pendry, J.B., Basov, D.N., Zhang, X.: Terahertz magnetic response from artificial materials. Science 303(5663), 1494–1496 (2004)
6. Moser, H.O., Casse, B.D.F., Wilhelmi, O., Saw, B.T.: Terahertz response of a microfabricated rod split ring resonator electromagnetic metamaterial. Phys. Rev. Lett. 94, 063901 (2005)
7. Casse, B.D.F., Moser, H.O., Lee, J.W., Bahou, M., Inglish, S., Jian, L.K.: Towards three-dimensional and multilayer rod- split-ring metamaterial structures by means of deep x-ray lithography. Appl. Phys. Lett. 90 (2007)
8. Marqués, R., Martín, F., Sorolla, M.: Metamaterials with Negative Parameters Theory, Design, and Microwave Applications. John Wiley & Sons, Inc. (2007)
9. Martin, F., Falcone, F., Bonache, J., Marques, R., Sorolla, M.: Split ring resonator based left handed coplanar waveguide. Appl. Phys. Lett. 83, 4652–4654 (2003)
10. Martin, F., Falcone, F., Bonache, J., Lopetegi, T., Marques, R., Sorolla, M.: Miniaturized CPW stop band filters based on multiple tuned split ring resonators. IEEE Microwave and Wireless Components Letters 13, 511–513 (2003)
11. Garcia-Lamperez, A., Salazar-Palma, M.: Dual band filter with split-ring resonators. In: 2006 IEEE MTT-S International Microwave Symposium Digest, pp. 519–522 (2006)
12. Lai, X., Liang, C.H., Su, T., Wu, B.: Novel dual-band microstrip filter using complementary split-ring resonators. Microwave and Optical Technology Letters 50(1), 7–10 (2008)

13. Fan, J.W., Liang, C.H., Wu, B.: Dual-band filter using equal-length split-ring resonators and zero-degree feed structure. Microwave and Optical Technology Letters 50(4), 1098–1101 (2008)
14. Genc, A., Baktur, R.: Miniaturized dual-passband microstrip filter based on double-split complementary split ring and split ring resonators. Microwave and Optical Technology Letters 51(1), 136–139 (2009)
15. Liu, H.W., Shen, L., Guan, X.H., Huang, D.C., Lim, J.S., Ahn, D.: Compact dual-band bandpass filter using octagonal split-ring resonators with side-coupled stubs. Microwave and Optical Technology Letters 53(5), 1169–1171 (2011)
16. Yuandan, D., Itoh, T.: Miniaturized dual-band substrate integrated waveguide filters using complementary split-ring resonators. In: 2011 IEEE MTT-S International Microwave Symposium, pp. 1–4 (2011)
17. Su, T., Zhang, L.J., Wang, S.J., Li, Z.P., Zhang, Y.L.: Design of dual-band bandpass filter with constant absolute bandwidth. Microwave and Optical Technology Letters 56(3), 715–718 (2014)
18. Geschke, R.H., Jokanovic, B., Meyer, P.: Filter parameter extraction for triple-band composite split-ring resonators and filters. IEEE Transactions on Microwave Theory and Techniques 59(6), 1500–1508 (2011)
19. Dong, Y., Wu, C.T.M., Itoh, T.: Miniaturised multi-band substrate integrated waveguide filters using complementary split-ring resonators. Microwaves, Antennas & Propagation, IET 6(6), 611–620 (2012)
20. Borazjani, O., Nosrati, M., Daneshmand, M.: A novel triple notch-bands ultra wideband band-pass filters using parallel multi-mode resonators and CSRRs. International Journal of RF and Microwave Computer-Aided Engineering 24(3), 375–381 (2014)
21. Jia-Sheng, L.M.J.: Microstrip Filters for RF/Microwave Applications. John Wiley & Sons, Inc. (2001)
22. Gupta, K.C., Garg, R., Bahl, I., Bhartis, P.: Microstrip lines and slotlines. Second Edition. Artech House, Boston (1996)
23. Temes, G.C., Mitra, S.K.: Modern filter theory and design. Wiley, New York (1973)